Tunable Optical Modulator by Coupling a Triboelectric Nanogenerator and a Dielectric Elastomer

*Xiangyu Chen, Xiong Pu, Tao Jiang, Aifang Yu, Liang Xu, and Zhong Lin Wang**

A conjunction system based on triboelectric nanogenerator (TENG) and dielectric elastomer actuator (DEA) is a promising demonstration for the application of TENG in the field of electronic skin and soft robotics. In this paper, a triboelectric tunable smart optical modulator (SOM) has been proposed based on this TENG-DEA system. The SOM has a very simple structure of an elastomer film and electrodes made of dispersed silver nanowires. Owing to the voltage induced rippling of the elastomer, the output of the TENG for a contact-separation motion at a velocity ranging from 0.5 to 10 cm s^{-1} can decrease the SOM's transmittance from 72% to 40%, which is enough for realizing the function of privacy protection. Meanwhile, an effective operation method is also proposed for this SOM. By serially connecting an accessory DEA to the SOM, an external bias voltage can be applied on the SOM to tune its "threshold" voltage and the output from TENG can smoothly regulate the transmittance on the basis of the bias. The proposed operation method has excellent applicability for all DEA-based devices, which can promote the practical study of TENG-DEA system in the field of micro-electro-mechanical system and human–robots interaction.

1. Introduction

In recent years, the concept of self-powered systems, which can harvest and utilize renewable energy from ambient environment, have been proposed and tested for realizing portable and self-sustainable electronics systems with various functions.[1] In comparison with other renewable energy techniques such as solar cell or pyroelectric harvesters, triboelectric nanogenerator (TENG) technique that can directly convert various mechanical motions into electrical energy is more attractive due to its advantage of simple fabrication, low cost, and extensive availability of the target resource.[2] Ever since its first report in 2012, a variety of breakthroughs have been made to improve the efficiency and the reliability of TENG, while the energy conversion efficiency reaches up to 50%–85% and the area power density reaches up to 500 W m^{-2}.[1,2] By employing TENG as either power supplier or regulating input, a series of self-powered and multi-functional electronics systems with both high effectiveness and excellent human/environment-interactive capability have been intensively investigated, including various wearable electronics, wireless sensors, and healthcare monitors.[3] The dramatic development of the efficiency of the TENG not only allows it to power some microelectronic system and functionalized sensors but also makes it possible to serve as high voltage source to drive or control some electromechanical systems.[4,5]

The application of TENG technique in the field of electromechanical systems may have several preconditions. First, the targeted system is better to be a voltage tunable system, which is suitable for the TENG's characteristic of large output voltage and low output current. Second, the terminal system for TENG should have rather high internal resistance, which can help TENG to maintain a high output voltage. The dielectric elastomer actuator (DEA) based on stretchable insulating elastomers has attracted extensive attention owing to its promising applications in artificial muscle, wearable electronics, and so on.[6,7] Under the high external electric field, the dielectric elastomers show significant shape deformation due to the effect of Maxwell force and such deformation can be utilized to realize various actuated motions. DEA requires a high driving voltage, while the device itself exhibits significant capacitor characteristic with a very high internal resistance.[7] These features make DEA to be a good companion for TENG. The conjunction system of TENG-DEA can produce a lot of interesting and practical applications in the field of smart actuators and wearable electronics.[5] However, the DEA devices show no significant deformation until a very high external voltage (few thousands volts) is applied.[7] Accordingly, the output signal from TENG still encounters a bottleneck for the effective operation of the DEA. The decrease of the elastomer thickness for DEA may reduce the operation voltage, whereas it can also increase the leakage current and thus suppress the output voltage from TENG. Therefore, it is quite necessary to design some specialized operation method for TENG to effectively regulate the performance of the DEA.

In this study, we have demonstrated a triboelectric tunable smart optical modulator (SOM) based on the TENG-DEA conjunction system. By using nanowire networks with optimized density to form the electrodes for DEA, the applied external

X. Chen, X. Pu, T. Jiang, A. Yu, L. Xu, Z. L. Wang
Beijing Institute of Nanoenergy and Nanosystems
Chinese Academy of Sciences
National Center for Nanoscience and Technology (NCNST)
Beijing 100083, P. R. China
E-mail: zhong.wang@mse.gatech.edu
Z. L. Wang
School of Materials Science and Engineering
Georgia Institute of Technology
Atlanta, GA 30332-0245, USA

DOI: 10.1002/adfm.201603788

electric field can generate a series of the localized surface deformation on the elastomer film, which can finally result in the changing of the light transmission through the elastomer due to the refraction effect. Accordingly, the light transmission through the device can be directly modulated by a simple contact-separation motion. The prepared tunable SOM can be a good demonstration for further application of TENG in fields of privacy protection and other optical devices. More importantly, a specialized driving method was designed for this SOM, by which TENG can smoothly modulate the transmittance of SOM with the help of a high voltage source and an accessory DEA. The proposed operation method is suitable for all the elastomer-based devices and it has the potential to be widely applied in the field of wearable electronics and soft robotics.

2. Results and Discussions

2.1. SOM System Based on Single-Electrode TENG

Figure 1a shows the design and the component of the SOM system based on the integrated TENG and DEA system. A single-electrode TENG using contact-separation working mode is fabricated and employed as the power source of the SOM system,[8] whereas the contact layers are Kapton film and Al foil. As introduced in our previous study, the contact-separation motion of the Kapton film can control the mechanical strain of the elastomer film, where the motion itself can serve as both the power supplier and trigger signal for the deformation of the elastomer.[5] In order to increase the surface charge density induced from contact-electrification and further enhance the output performance of the TENG, a high surface area is achieved by covering the Kapton film with a series of nanopatterned structure using inductively coupled plasma (ICP) reactive-ion etching. Figure 1b shows scanning electron microscopy (SEM) images of the Kapton thin film surface, where a series of uniformly distributed nanoparticle arrays structure can be observed with an average diameter of about 300 nm (Figure 1b). As also shown in Figure 1a, the DEA device is prepared by applying nanowire electrode on both top and bottom sides of an elastomer film. Under the activation of the TENG, the nanowire electrode can manipulate the optical transmittance through the elastomer and thus alter the observation image through the film, which can be considered as a privacy protection device. The modulated optical image through this SOM device is shown in Figure 1c (Video S1, Supporting Information), where a transparent film turns into a frosted film under the drive of TENG.

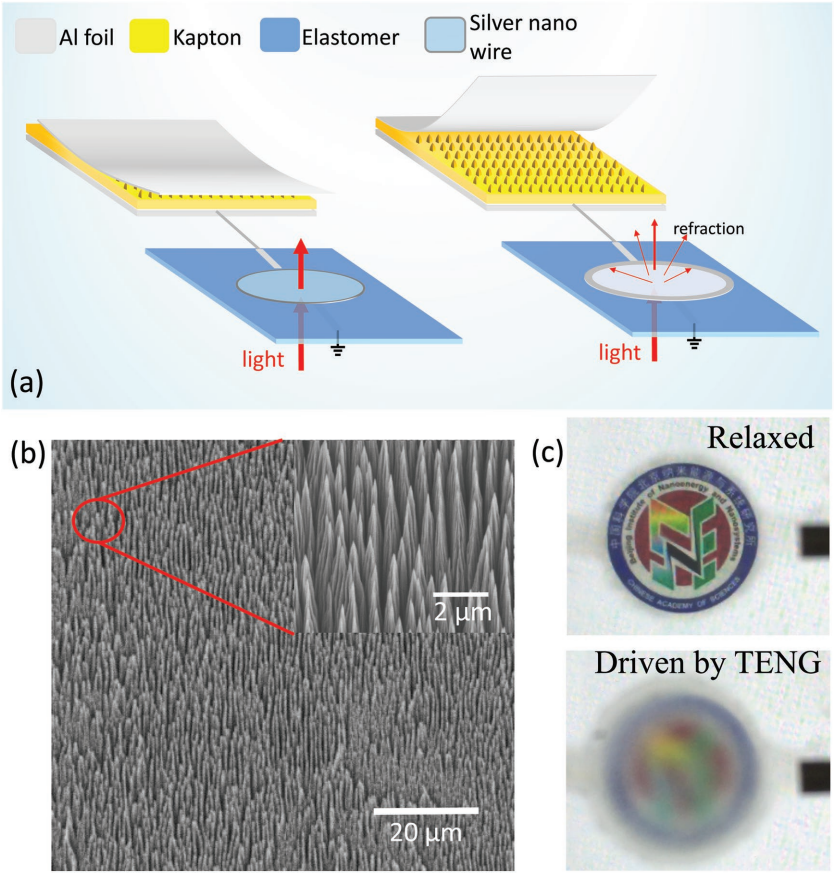

Figure 1. a) A sketch of the triboelectric tunable SOM based on TENG-DEA system, where the transmittance of the elastomer film can be controlled by the contact-separation motion. b) SEM image of the Kapton film after ICP treatment, where the nanopatterned structures are applied on the surface in order to enhance the contact-electrification process. c) Changes of opacity under the drive of TENG, which shows the control of in-line transmittance by using contact-separation motion. The logo is placed at a position of 3 cm behind the SOM film.

When an Al foil contacts with the Kapton film (see **Figure 2**a), the positive and negative surface charges are induced on the surface of foil and Kapton, respectively. The successive separation motion results in a high potential drop established between Kapton film and the ground (the positive charges remain on the surface of Al foil), which will finally result in the hole accumulation on the Al electrode beneath the Kapton film. Accordingly, the SOM system connected between Al electrode and ground will endure this potential drop due to its capacitance characteristic and the deformation strain on the nanowire electrodes will be activated. When the Al foil return to the contact position, the positive charges on the surface of Kapton film are neutralized by the negative charges on the surface of Kapton and the potential drop between Al electrode and the ground will be vanished. For the electrical measurement of the prepared single-electrode TENG, two plates (top and bottom) are designed to be the moving objects, as explained later in the experimental section. The Al foil is attached to the top plate, which is guided by a linear motor in the vertical direction of the bottom plate. At the beginning, two plates are aligned with each other and the separating displacement of the top plate can be controlled by the linear motor with a position resolution of 1 mm. The separating movement is in a

Adv. Funct. Mater. 2016,
DOI: 10.1002/adfm.201603788

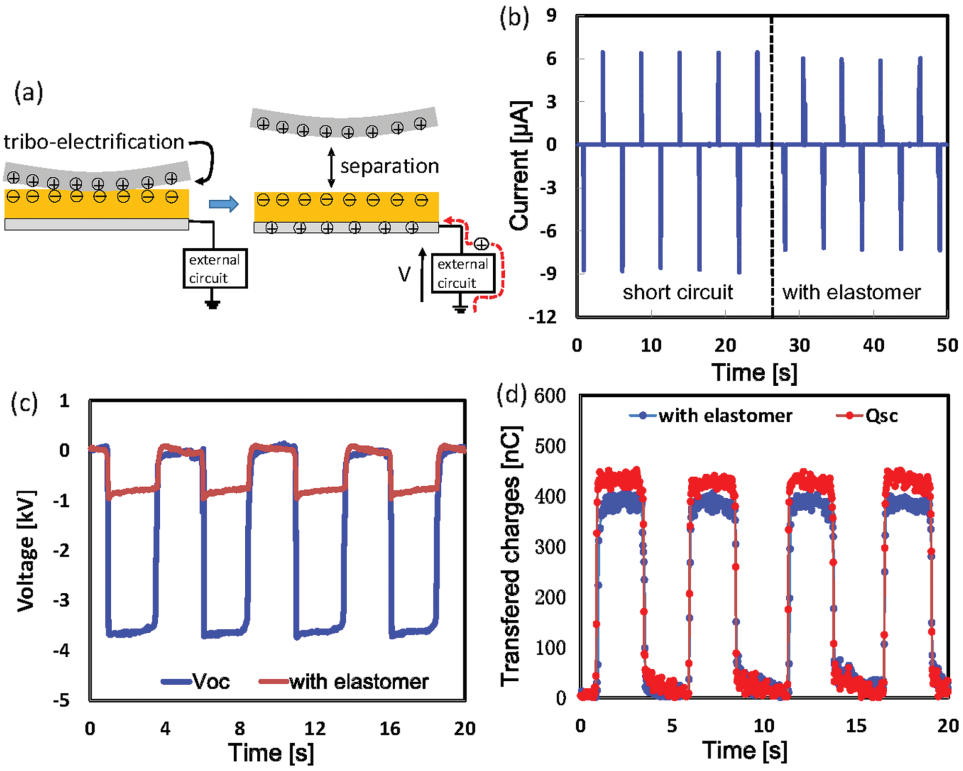

Figure 2. Output performance from single-electrode TENG: a) the illustration of the working principle of the single-electrode TENG. b) Measured I_{SC} from TENG and the output current with the optical DEA sample. c) Measured V_{OC} from TENG and the output voltage with the optical DEA sample. d) Transferred charges of the TENG device with and without the optical DEA. Here, the tribo-surface is about 100 cm^2.

symmetric acceleration–deceleration mode with an acceleration rate of ±20 m s^{-2} and the velocity can be changed optionally by a control system. The open-circuit voltage (V_{OC}) and short-circuit current (I_{SC}) are measured by an electrometer with a very high internal resistance and the results can be seen in Figure 2a,b. Meanwhile, the output current and output voltage from TENG to the elastomer based device are also measured, as can be seen in Figure 2b,c. For the tribo-surface of 100 cm^2, the maximum output voltage measured by electrometer can reach 3600 V, while the generated voltage drop on the SOM device by TENG is about 1000 V. In this experiment, we modified an electrostatic voltmeter (Monroe ME-297) and used it to catch the dynamic performance of the Voc. The Monroe ME-297 voltmeter is usually used for checking the surface potential of the electrified materials and it has a very high internal resistance, which can help to maintain the tribo-induced charges on TENG. Moreover, numerical calculations for the single-electrode TENG under constant motion velocity were performed with the help of finite element method (FEM),[4,5] in order to better understand the output performance of the TENG. The results can be found in Figure S1a–c (Supporting Information). (The detailed calculation parameters are listed in Table S1 (Supporting Information).) Here, with a short-circuited current value of 7 μA, the open-circuit voltage value can reach 9000 V. The numerical calculation confirms that the observed high V_{OC} of the TENG is within an acceptable range and this V_{OC} is related to the electrostatic field in the isolated condition, which will be decreased quickly if the electrostatic isolation is disturbed. In our experiment, the elastomer film has rather large pre-strain ratio (λ = 10) and the thickness of the film is about 25 μm. The transferred charges from TENG to the elastomer film and from TENG to the ground (short-circuited) were also tested (see Figure 2d). The transferred charges with the elastomer film are slightly decreased in comparison with that of the short-circuit condition, which is because that the inherent capacitance of TENG shares part of the tribo-induced charges.[5]

The decrease of the voltage output with the elastomer sample in Figure 2c is related to the capacitance changing of the whole system. The leakage current through the elastomer (or along the surface of the elastomer) only causes some slight decrease of the voltage drop after it reaches the maximum value (see Figure 2c). As analyzed by previous study,[4,5] the voltage (V_{max}) on the elastomer and the V_{OC} are given as: (Q_{SC} stand for the short-circuit transferred charges of the TENG when $x = x_{max}$) $V_{max} = C_T V_{OC}/(C_T + C_L) = Q_{SC}/(C_T + C_L)$, where C_T and C_L are the capacitance value of TENG and elastomer. With the elastomer sample, the total capacitance value of the system increased, while the tribo-induced charges are theoretically the same. Accordingly, the established voltage drop significantly decreased in Figure 2c. On the other hand, the transferred charges (Q_{max}) as well as the current between TENG and elastomer are decided by the capacitance difference between them (C_T and C_L). That is, $Q_{max} = C_L Q_{SC}/(C_T + C_L)$. Based on the transferred charges in Figure 2d, it can be figured out that the C_T of TENG is ≈1/10 of the C_L of the elastomer. In this case, the output voltage drop with elastomer should be about

one-tenth of the V_{OC}, which is different from that we observed in Figure 2c. It is important to note that this analysis did not consider the effect of the ionization of air at extremely high voltage (V_{OC}) and the influence of the internal capacitance of the measuring instruments under open-circuit condition. Both two effects may consume the tribo-induced charges and cause the measured V_{OC} to be smaller than the theoretical V_{OC} value ($=Q_{SC}/C_T$).

In current study, the core element of the SOM device consists of a thin nanowire network to serve as the electrode of the device. The SEM images of the silver nanowire with different density are shown in Figure S2a–c (Supporting Information), where the different densities (electrode 1, 2, and 3) are achieved by changing the splashing numbers. Here, every splash will approximately generate a nanowire network with a density of 5 mg m^{-2}. The working principle of this SOM device is similar to the operation of common DEA and the schematic explanation of the working principle is shown in **Figure 3**a. When a voltage is applied across the thickness of an elastomer, Coulombic attraction between the opposing charges on top and bottom electrodes results in a spatially uniform Maxwell stress that compresses the dielectric.[9] The Maxwell stress (P) is generated from the electrostatic attraction between the charges on the opposing electrodes, which can be given as: $P=-\varepsilon E^2$, where E is the electrical field strength and ε is the permittivity of the elastomer layer.[9] Accordingly, the elastomer film caught in the middle of the two electrodes is squeezed to become thinner in response to the Maxwell stress. When two electrodes of nanowire network are employed instead of the flat and continuous electrodes, a series of macroscopic compression and squeeze of the elastomer will be induced on its surface due to the electrostatic force exerted on each nanowire. Accordingly, many localized deformations ("wrinkles" in nanoscale) will be generated on the surface of the elastomer (see Figure 3a). This macroscopic surface deformation can alter the optical transmittance due to a series of refraction process on the surface. Thus, the device can be considered as an optical modulator to manage the observation image through the elastomer film. In this experiment, we found that the density of the nanowire network can significantly change the optical manipulating

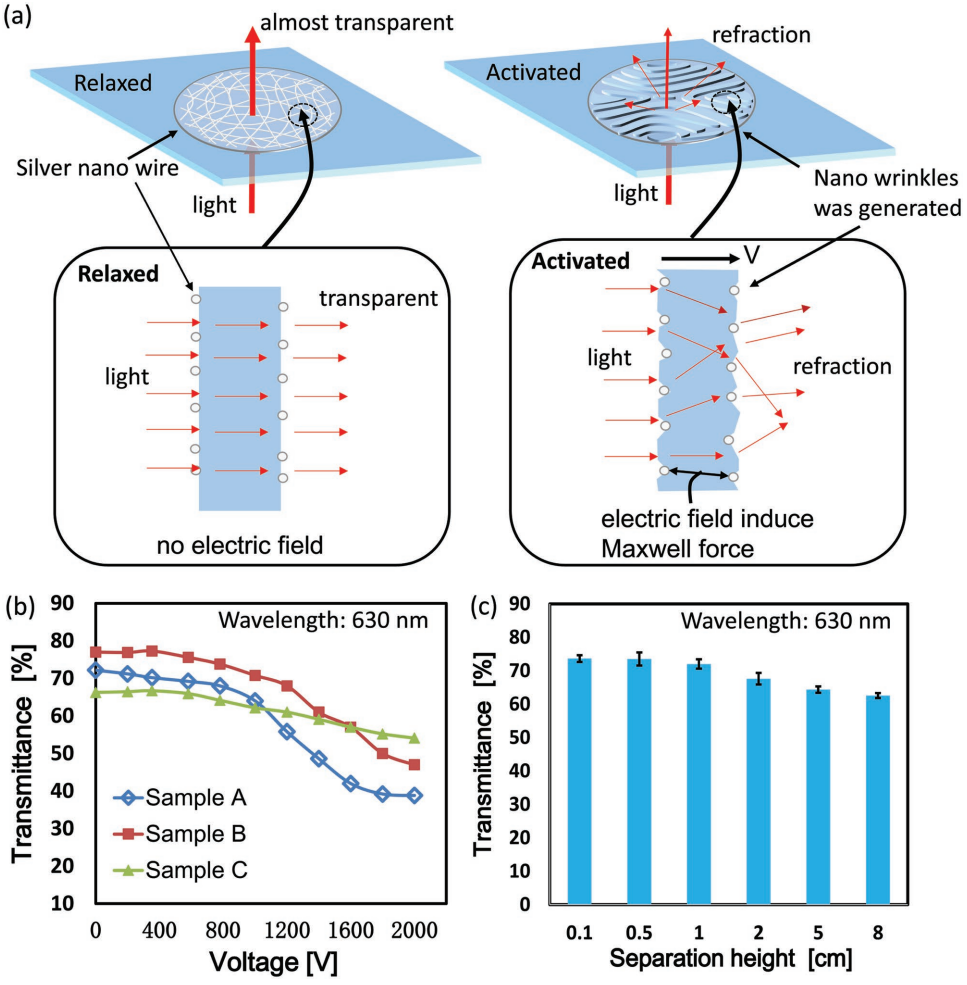

Figure 3. a) The sketch and the explanation of the working principle of the SOM, where silver nanowires can generate nano-wrinkles to change the transmittance. b) Optical transmittance at a wavelength of 630 nm as a function of electrical voltage for three different samples. c) The transmittance of the sample A under the drive of TENG, where the separation height was changed from 0.1 to 8 cm.

Adv. Funct. Mater. **2016**,
DOI: 10.1002/adfm.201603788

capability of the device. Accordingly, in order to determine the optimized composition of the SOM sample, we designed three kinds of samples with different combinations of the electrodes: sample A (electrode 1 and electrode 2) sample B (electrode 1 and electrode 3), and sample C (electrode 1 and electrode 1). The structure and the composition of each sample are illustrated in Figure S2d (Supporting Information). By coupling two nanowire electrodes with different densities, the optical manipulating capability can be significantly enhanced.

The in-line optical transmittances of all three samples at a wavelength of 630 nm as a function of electrical voltage are shown in Figure 3b. Here, the transmittance can be tuned continuously between 70% and 40% by controlling the actuation voltage (see Figure 3b). As can be seen in Video S1 (Supporting Information), the transmittance value of 40% is enough to block the observation through the film and the image information under the elastomer film can be protected. The optical transmittance data at all wavelengths for three different samples are shown in Figure S3a–c (Supporting Information). Without the nanowire electrodes, the dielectric layers have an in-line transmittance about 90%, where the light lost is attributed to the surface reflection effect. After the deposition of two nanowire electrodes, the transmittance decreases to 65%–75%. The decrease is mainly caused by scattering from the metal nanowires, rather than any optical absorption. In sample A, the in-line transmittance drops to 40% at a voltage of about 1.8 kV, which is the best result we can obtain from the three samples. The combination of two nanowire electrodes with different density can significantly enhance the optical modulating capability, which is quite an interesting result. The detailed mechanism may still require further analysis. We can anticipate that the unbalanced density of nanowire may constrain the lateral expansion of the elastomer film under activation and thus the electrostatic forces generate more displacements in the thickness direction, which can significantly enhance the refraction process through the film. It is important to note that the transmittance curve as a function of voltage has a nonlinear shape, particularly near the low voltage region (see Figure 3b). The existence of this nonlinear behavior is due to the quadratic dependence of Maxwell force on the electric field and it can be considered as a "threshold" voltage (about 800 V) for the significant changing of the transmittance. For the conjunction system of TEMG and SOM, this "threshold" voltage can impede the effective operation of the SOM by using TENG, since the output voltage from TENG to SOM is about 1000 V (see Figure 2c). The in-line optical transmittance of the sample A (our best sample) under the drive of single-electrode TENG are shown in Figure 3c, where the separation height of 8 cm can reduce the transmittance to be 60%. Furthermore, both the V_{OC} from single-electrode TENG and the output voltage with the elastomer sample has been measured according to different separation heights. The results can be seen in Figure S3d (Supporting Information), where the motion velocity is 1 m s^{-1}. Here, the output voltage from TENG increases to be more than 500 V, when the separation height is larger than 1 cm. Accordingly, as shown in Figure 3c, the transmittance of the SOM starts to show notable decrease after the separation height is larger than 1 cm. If the separation height is increased to be larger than 5 cm, the increased amplitude of the output voltage is decreased. Therefore, the transmittance changing in the region larger than 5 cm shows slight difference. It has also been found that the motion velocity shows little influence on the deformation (see Figure S3e, Supporting Information), which is not surprising since the tribo-charges need a long time (at least tens of seconds) to relax in the air. The experiments are all repeated for more than five times and the generated error bars are shown in Figure 3c and Figure S3d (Supporting Information), respectively. The transmittance changing powered by TENG is not appealing for a reliable privacy protection device. Thus, it is quite necessary to realize some optimized operation method for TENG to regulate the deformation of the DEA.

2.2. An Effective Operation Method for TENG-DEA System

As can be seen in Figure 3b, the transmittance decreases almost linearly with the increase of the applied voltage in the region from 800 to 1800 V. If a bias voltage can be pre-applied on the SOM to overcome its "threshold" voltage (800 V), the output signal from TENG can smoothly modulate the optical transmittance of the SOM. The proposed operation method is schematically illustrated in Figure S4 (Supporting Information). Here, two DEA devices (DEA1 and DEA2) are connected in series, while the output signal of the single-electrode TENG is applied at the middle position of the serial DEAs. A high external voltage is applied across the serial DEA system, where the generated voltage drop on each device (V_1, V_2) is approximately decided by the capacitance value of each DEA. Here, $V_1 = V_{ex}C_2/(C_1+C_2)$ and $V_2 = V_{ex}C_1/(C_1+C_2)$, where C_1 and C_2 are the capacitance value of DEA1 and DEA2, respectively. The output signal (V_T) from TENG increases the voltage drop on DEA1, while decreases the voltage drop on DEA2, as shown in Figure S4 (Supporting Information). Finally, $V_1' = V_1 + V_T$ and $V_2' = V_2 - V_T$. The total potential drop across the whole serial DEAs system is fixed to be the V_{ex} from power source (see Figure S4, Supporting Information). Meanwhile, the TENG can serve as the potential modulator to manage the potential distribution on each DEA sample in this serial structure. It is very important to note that the TENG device cannot be directly connected to the voltage source in parallel, since the potential drop between two output ends of the voltage source always fixes. Moreover, the internal circuit of the power source would shunt the tribo-charges and the TENG cannot even instantaneously increase the voltage drop applied on the DEA device. On the other hand, if the TENG is serially connected between voltage source and DEA sample, the extremely high internal resistance of TENG will occupy almost all the potential drop applied from voltage source and the operation of the DEA is still not smooth. Hence, this serial DEAs structure is so far the best option that allows TENG to effectively regulate the actuation behavior of the DEA sample. The previous studies related to the electrical modulation function of the TENG are mainly focused on the utilization of TENG as a "gate" input to boost current flow in the transistors,[10] namely, the tribotronic effect. The direct modulation of the potential distribution in a serial system by using TENG has not yet been considered. Hence, this special operation method for serial DEA system can be a new approach

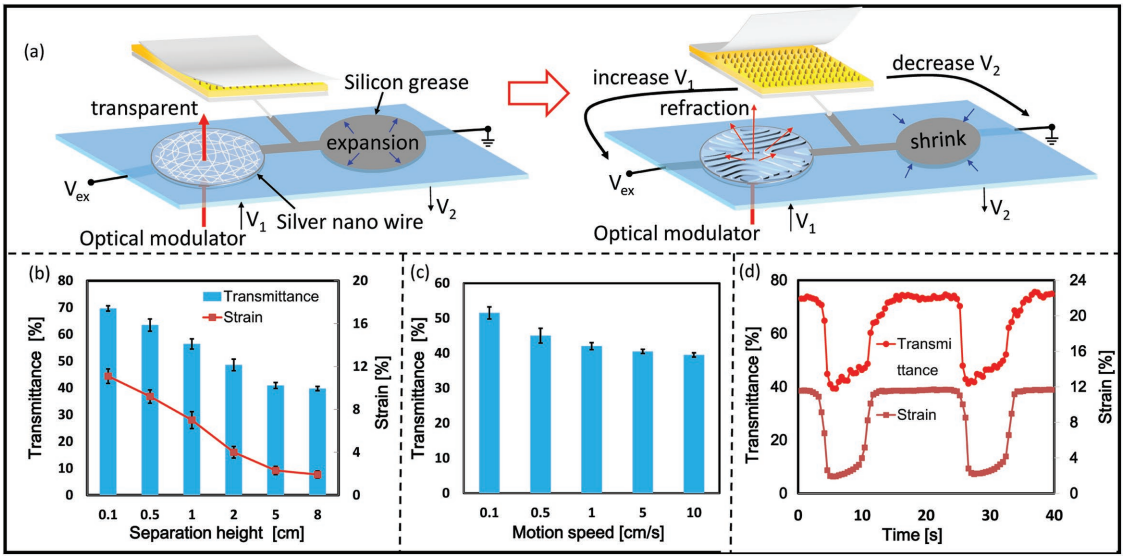

Figure 4. a) The SOM driven by the new method, where the output from TENG will lead to the shrinkage of the common DEA sample and the enhancement of SOM. b) The change of the transmittance of the SOM and the change of the activated strain of the common DEA sample. c) The change of the transmittance at different motion speed. d) The transient response of the SOM and the common DEA sample under the drive of continuous contact-separation motion. Here, the transmittance is checked at a wavelength of 630 nm.

for exploring the regulation and administration function of the TENG in the field of tribotronics.

Based on the operation method proposed in Figure S4 (Supporting Information), a more efficient SOM system was prepared, as can be seen in **Figure 4**a. An accessory DEA device using silicon grease as the flat and continuous electrode[5] has been fabricated and connected with the SOM in series, as shown in Figure 4a. The external voltage (V_{ex}) of 1400 V is applied on the whole serial DEAs system in Figure 4a. By using the electrometer to check the potential drop on each DEA device, we found that the potential drop on SOM part is larger than 800 V (the threshold value for optical modulation) and that on the accessory DEA device is about 600 V. In this case, the output voltage from TENG will further increase the potential drop on SOM to be larger than 1600 V. Accordingly, significant transmittance changing can be observed from SOM under the control of contact-separation motion. On the other hand, the accessory DEA device next to the SOM shows significant expansion strain under the V_{ex}. During the separation motion of the TENG, the potential drop on this DEA reduces to about −200 V. Therefore, the shrinkage of the accessory DEA can be observed with the separation motion. The detailed working principle of this serial SOM system can be seen in Figure 4a. The change of the transmittance through the SOM and the shrink of the actuated strain on the accessory DEA device are both measured, as can be seen in Figure 4b. The separation distance of 8 cm can reduce the transmittance to be 40%, which is enough to satisfy the purpose of privacy protection (see Figure 1c, and Video S1, Supporting Information). Meanwhile, the actuated strain of the accessory DEA device decreases from 11% to 1.8% with separation distance of 8 cm. As can also be seen in Figure 1c and Video S1 (Supporting Information), the transmitted optical signal through the film is broadened after the modulation of the SOM. It is thus necessary to check the haze effect of the SOM. As can be seen in Figure S5a (Supporting Information), the laser spot experiences a strong scattering effect through the activated SOM sample and the light intensity in the central region of the laser spot decreases significantly. The haze of the SOM can be briefly calculated through a simple system shown in Figure S5b (Supporting Information). Here, a circular mask is used to block the scattered light, while the photometer can detect the change of the intensity through the film. The haze can be approximately given as: $(I_{total} - I')I_{total} \times 100\%$, where I_{total} is the original intensity before the activation of the SOM and I' is the remaining light intensity after the activation of the SOM. The change of the haze with different separation height of the TENG can be seen in Figure S5c (Supporting Information). The haze measurements confirm that the change of the transmittance is mainly due to the microscopic refraction processes induced by silver nanowires.

Moreover, the influences of the motion velocity to the transmittance changing are also measured and shown in Figure 4c, where the separation distance is fixed to be 8 cm. It has been found that the system works stably within the contact-separation velocity ranging from 0.5 to 10 cm s^{-1}, which is the common motion velocity for the object in the daily life. The further increase of the velocity shows no significant influence to the results, while the actuation performance of SOM would be slightly suppressed for the extreme slow velocity (0.1 cm s^{-1}). The dynamic performance of this serial SOM system has also been studied (see Figure 4d), where transient changing of the transmittance and the actuated strain are both recorded in the time domain (sampling rate is 0.5 s). It is necessary to note that a higher sampling rate is required for getting more detailed dynamic performance of the transmittance changing. We are designing more advanced measuring system for the further study of this SOM system. Here, the motion velocity and the separation distance are 10 cm s^{-1} and 8 cm, respectively. As

Adv. Funct. Mater. **2016**,
DOI: 10.1002/adfm.201603788

can be seen in Figure 4d, the transient performance of this SOM system can follow the separation motion of the TENG very well. For each separation motion, the change of the transmittance is rather rapid and the transmittance can be reduced to the minimum value in less than 0.5 s. The slight increase of the transmittance after the triboelectric excitation is mainly due to the leakage current through the film and it can improve by employing some more advanced elastomer materials with better insulating performance. Another video material about the operation of this serial SOM system is prepared in Video S2 (Supporting Information). For each situation in Figure 4b,c, the experiments have been repeated for more than five times, in order to confirm the repeatability, and the generated error bars are also exhibited in the figures. These results confirm the possibility to utilize TENG technique to provide a safe, efficient, and precise driving of SOM devices.

As shown in Figure 4a–d, the smooth regulation of the transmittance through SOM system by using TENG device confirms the effectiveness of the new operation method for DEA-based system. The quadratic dependence of Maxwell force on the electric field is a common behavior for all elastomer-based actuators. Accordingly, the electrostatic reaction (expansion strain, longitudinal stress, and so on) at the low voltage region (<1000 V) is quite insignificant for all these devices and the remarkable response to the applied voltage changing will appear only after a "threshold" voltage value has been exceeded.[6,7] In this case, the proposed operation method in this paper can be further applied for all the other elastomer-based devices and thus the conjunction system of TENG-DEA can serve as a more efficient medium for human–machine interfacing. In order to further demonstrate the practicability of this operation method to the elastomer-based devices, we present a triboelectric regulated electroluminescence (EL) device, in which TENG can control the intensity of a stretchable EL device. We fabricate the EL device using a widely available phosphor, zinc sulfide (ZnS) doped with Cu.[11] In order to make the device stretchable, we use ZnS in the form of powders (Science and Technology Ltd., Shenzhen, China). The same transparent elastomer film and the silver nanowire electrodes in SOM device are directly employed for the fabrication of the EL device. The structure of the EL device as well as the built-up triboelectric modulation system are both shown in **Figure 5**a. An accessory DEA device using silicon grease as the electrode is connected with EL device in the same way as the case of the SOM system (see Figure 4a). The photograph of the fabricated devices and the electroluminescent performance are shown in Figure 5b, where the device is transparent except for parts covered with phosphor and grease electrode. The luminance of the device depends on the amplitude of the applied voltage (Figure 5c). In more details, the device starts to luminesce at a voltage about 0.6–0.9 kV and becomes much brighter at a voltage larger than 2 kV. As can be seen in Figure 5c, the similar "threshold" like behavior can be observed and thus the new operation method is suitable for this case. In Figure 5a, the external voltage of 1800 V is pre-applied on the whole serial DEA system. Accordingly, the potential drop on EL part is checked to be around 1100 V and the accessory DEA part is about 700 V. The operation of this serial EL system can be seen in Figure 5d and Video S3 (Supporting Information). The luminance changing during the contact-separation motion has been recorded, as shown in Figure 5d, where the separation distance of 8 cm can induce a luminance of 1.4 cd m^{-2}. Hence, the output voltage from TENG further increases the potential drop on EL device to be larger than 2400 V. On the other hand, if the same TENG output is directly applied on the EL device without the help of external bias, the generated luminance is only about 0.3 cd m^{-2}, which is difficult to be clearly observed by human eyes. It is also interesting to find out that the output voltage from the TENG in the EL case is larger than that in the previous SOM's case. The increase of the film thickness results in the increase of the total resistance and the output voltage from TENG, which is determined by the external resistance,

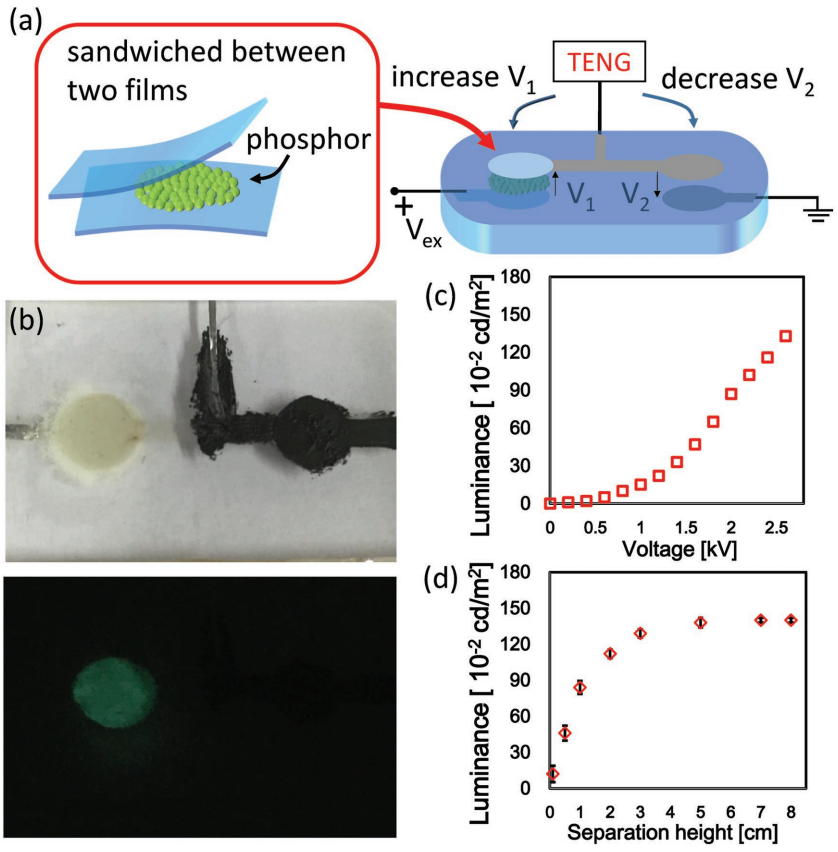

Figure 5. a) A sketch of another application of TENG-DEA system for demonstrating the capability of special operation method. The EL device replaced SOM in the serial system, where the commercial ZnS phosphor was directly buried in between two elastomer films to form the EL device. b) The photograph of the prepared sample and the generated luminescent behavior. c) The luminance under the driving voltage. d) The luminance under the drive of TENG.

can be relatively increased.[5,9] The performance of the reported EL prototype can be further optimized by employing some advanced phosphor component. Meanwhile, the smooth operation of this EL device using TENG further confirms the applicability and the effectiveness of the proposed operation method for the TENG-DEA conjunction system. Based on this unique operation method, the regulating capability of the TENG for the DEA-based devices can be significantly amplified and an effective control of the DEA-based system can be achieved. A series of continuous works can be done to further promote the performance and the function of the TENG-DEA conjunction system on account of this new operation method.

3. Conclusions

In summary, by coupling a single-electrode TENG and a DEA with nanowire electrodes, we have demonstrated a novel triboelectric tunable SOM system. The separation motion of an Al foil with the size of 100 cm^2 can decrease the transmittance from 72% to 40% for the SOM sample, which is enough for hiding the image information behind the SOM. The simple structure, ease of operation, and the stretchable texture of this SOM system suggest that it can be potentially applied in the field of smart window, laser beam system, projector screen, privacy protection, and so on. Meanwhile, in order to realize an effective control of this SOM, a specialized operation method is also proposed. By serially connecting an accessory DEA to the SOM, an external voltage bias is applied on the SOM to overcome its "threshold" voltage and after that the output from TENG can smoothly control the transmittance of the SOM on the basis of this voltage bias. The proposed driving method can be universally applied to all the DEA-related devices. Accordingly, an elastomer-based EL device is fabricated and replaces the SOM in the serial system. The significant enhancement of the luminescence by using TENG has also been observed, which confirms the excellent applicability of this operation method for DEA-related device. The proposed operation method can strongly facilitate the interaction between the TENG and DEA, while it is also a new demonstration of the regulation function of the TENG for the field of tribotronics. The SOM system and the specialized operation method proposed in this paper can further promote the practical study of TENG-DEA system for the field of MEMS/NEMS, human–robots interaction, and internet of things.

4. Experimental Section

Fabrication of Single-Electrode TENG: In the measurement, the single-electrode TENG is structurally composed of a two plates with plastic slides as the supporting substrates to ensure the surface flatness (Figure 1a). Two Al foils with rectangular shape were attached on the surface of both the plates, where the foil on the bottom plate serve as the output electrode and the foil on the top plate plays the role of a tribo-surface. The Kapton adhesive tape (thickness ≈ 50 μm) with nanopatterned surface was purposely chosen as the triboelectric layers adhered to the Al foil on the bottom plate, where the effective tribo-surface for contact-separation motion is about 100 cm^2 (10 cm × 10 cm) . The Kapton film with nanopatterned surface was fabricated by inductively coupled plasma (ICP) reactive-ion etching. Briefly, a 50 μm thick Kapton thin film (American Durafilm) was cleaned with methanol, isopropyl alcohol, and deionized water sequentially, and then blown dried with nitrogen gas. Subsequently, Ar, O_2, and CF_4 gases were introduced into the ICP chamber at a flow rate of 15, 15, and 35 sccm, respectively. The Kapton film was etched (plasma-ion acceleration = 100 W) for 20 min to obtain the nanowire array structure on its surface. The two plates were kept in parallel with each other, where the inner surfaces are in intimate contact.

Fabrication of SOM: Acrylic elastomers (0.25 mm thick, VHB 9473, 3M) were cut into 20 × 40 mm sheets. The elastomer sheet was first stretched with a pre-strain ratio ($\lambda = 10$) and then the film was fixed uniformly along a frame for the test. In this case, the pre-strain ration is defined as the ratio between area of the elastomer film after (A') and before (A) stretching ($\lambda = A'/A$). The circular area (diameter 1 cm) at the center of the film was coated with the silver nanowire networks on the upper and lower side (with the help of a circular mask). The silver nanowires (Nanjing XFNANO Materials Tech Co., Ltd.) with a diameter of 30 nm and a length of 100–200 μm were uniformly dispersed in the ethanol solution. The solution concentration is 1 mg mL^{-1}. The nanowire solution was splashed on the elastomer film through an air pump. Here, every splashing will approximately generate a nanowire network with a density of 5 mg m^{-2} in a region of 0.01 m^2 and the spray numbers can be controlled to change the density of the nanowire. The compliant electrodes (circular shape) for accessory DEA in the serial system were prepared by directly smearing graphite/silicone grease and curing agent onto the surface of the dielectric elastomers. The electrodes were connected to TENG or a high voltage supplier through a thin Al foil.

Fabrication of the Stretchable EL Device: The elastomer film with a pre-strain ratio of 10 was first attached on a frame. After that, ZnS powders were deposited homogeneously on the surface of the elastomer with the help of a mask, forming the phosphor layer. Then, the redundant phosphor powers as well as the mask were removed and after that another elastomer film with the same pre-strain ration was symmetrically covered on top of the phosphor layer to seal the devices. Finally, the silver nanowire network was splashed on the top and bottom of the sealed device to form the electrodes. During the real operation, aluminum foils were attached onto the nanowire electrode to provide electrical connection.

Characterization: The single-electrode TENG was driven periodically by a linear motor. The plate with the Al foil was fixed to a stationary stage, whereas the plate with only Kapton film can be moved by motor and thus contact-separation motion can be achieved. By employing a numerical control linear motor to drive the Kapton plate, the speed and the moving distance of the plate can precisely be regulated. The output performance of the single-electrode TENG was measured by an oscilloscope and Stanford Research Systems. A Monroe ME-297 electrometer and Keithley 4200 were used to detect the voltage and transferred charges of TENG, respectively. The transmittance in the range of 400–800 nm was detected by a spectrograph (HORIBA, iHR550). Luminance of the EL devices was measured by using a spectral photometer (Konica Minolta, CS-200).

Supporting Information

Supporting Information is available from the Wiley Online Library or from the author.

Acknowledgements

X.C. and X.P. contributed equally to this work. The authors acknowledge the support from the national key R&D project, the "thousands talents" program for pioneer researcher and his innovation team, China and National Natural Science Foundation of China (Grant Nos. 2016YFA0202704, 61405131, 51432005, 5151101243, and 51561145021).

Received: July 26, 2016
Revised: August 19, 2016
Published online:

[1] a) S. Xu, Y. Qin, C. Xu, Y. G. Wei, R. S. Yang, Z. L. Wang, *Nat. Nanotechnol.* **2010**, *5*, 366; b) M. D. Han, X. S. Zhang, B. Meng, W. Liu, W. Tang, X. M. Sun, W. Wang, H. X. Zhang, *ACS Nano* **2013**, *7*, 8554; c) G. T. Hwang, H. Park, J. H. Lee, S. Oh, K. I. Park, M. Byun, H. Park, G. Ahn, C. K. Jeong, K. No, H. Kwon, S. G. Lee, B. Joung, K. J. Lee, *Adv. Mater.* **2014**, *26*, 4880; d) J. H. Lee, K. Y. Lee, M. K. Gupta, T. Y. Kim, D. Y. Lee, J. Oh, C. Ryu, W. J. Yoo, C. Y. Kang, S. J. Yoon, J. B. Yoo, S. W. Kim, *Adv. Mater.* **2014**, *26*, 765.

[2] a) K. Y. Lee, H. Yoon, T. Jiang, X. Wen, W. Seung, S. W. Kim, Z. L. Wang, *Adv. Energy Mater.* **2016**, doi: 10.1002/aenm.201502566; b) J. W. Zhong, Y. Zhang, Q. Z. Zhong, Q. Y. Hu, B. Hu, Z. L. Wang, J. Zhou, *ACS Nano* **2014**, *8*, 6273; c) F. R. Fan, Z. Q. Tian, Z. L. Wang, *Nano Energy* **2012**, *1*, 328; d) X. Chen, M. Iwamoto, Z. Shi, L. Zhang, Z. L. Wang, *Adv. Funct. Mater.* **2015**, *25*, 739.

[3] a) G. Zhu, Y. S. Zhou, P. Bai, X. S. Meng, Q. S. Jing, J. Chen, Z. L. Wang, *Adv. Mater.* **2014**, *26*, 3788; b) W. Tang, T. Jiang, F. R. Fan, A. F. Yu, C. Zhang, X. Cao, Z. L. Wang, *Adv. Funct. Mater.* **2015**, *25*, 3718.

[4] a) D. Yang, D. Kim, S. H. Ko, A. P. Pisano, Z. Li, I. Park, *Adv. Mater.* **2015**, *27*, 1207; b) C. Zhang, W. Tang, Y. Pang, C. Han, Z. L. Wang, *Adv. Mater.* **2015**, *27*, 719; c) S. Niu, Y. Liu, Y. S. Zhou, S. Wang, L. Lin, Z. L. Wang, *IEEE Trans. Electron Devices* **2015**, *2*, 641.

[5] X. Chen, T. Jiang, Y. Yao, L. Xu, Z. Zhao, Z. L. Wang, *Adv. Funct. Mater.* **2016**, doi: 10.1002/adfm.201600624.

[6] a) C. H. Yang, B. Chen, J. Zhou, Y. M. Chen, Z. Suo, *Adv. Mater.* **2016**, *28*, 4480; b) S. Shian, D. R. Clarke, *Opt. Lett.* **2016**, *41*, 1298.

[7] a) S. Shian, K. Bertoldi, D. R. Clarke, *Adv. Mater.* **2015**, *27*, 6814; b) S. Bauer, S. Bauer-Gogonea, I. Graz, M. Kaltenbrunner, C. Keplinger, R. Schwödiauer, *Adv. Mater.* **2013**, *26*, 149; c) I. A. Anderson, T. Hale, T. Gisby, T. Inamura, T. McKay, B. O'Brien, S. Walbran, E. P. Calius, *Appl. Phys. A: Mater. Sci. Process.* **2010**, *98*, 75.

[8] S. Niu, Y. Liu, S. Wang, L. Lin, Y. S. Zhou, Y. Hu, Z. L. Wang, *Adv. Funct. Mater.* **2014**, *24*, 3332.

[9] Z. Suo, *Acta Mech. Solida Sin.* **2010**, *23*, 549.

[10] a) C. Zhang, W. Tang, L. Zhang, C. Han, Z. L. Wang, *ACS Nano* **2014**, *8*, 8702; b) C. Zhang, J. Li, C. Han, L. Zhang, X. Chen, L. Wang, G. Dong, Z. L. Wang, *Adv. Funct. Mater.* **2015**, *25*, 5625.

[11] a) A. Kitai, *Luminescent Materials and Applications*, Wiley, Chichester, UK **2008**; b) A. J. Bard, L. R. Faulkner, *Electrochemical Methods*, Wiley, New York **2001**.